Higher conductivity in doped ethylenedioxythiophene (EDOT) dimers with chalcogen-substituted end groups

Kota Onozuka, Tomoko Fujino*, Tatsuya Miyamoto, Takashi Yamakawa, Hiroshi Okamoto, Osamu Yamamuro, Hiroshi Akiba, Eiichi Kayahara, Shigeru Yamago, Hiroshi Oike and Hatsumi Mori*

1. General

Preparative gel permeation chromatography (GPC) was performed on JAIGEL 1HR and 2HR polystyrene columns (Japan Analytical Industry) with chloroform as the eluent.

2. Apparatus

Proton and carbon nuclear magnetic resonance spectra (^{1}H and ^{13}C NMR) were recorded on a JEOL JNM-AL300 (^{1}H NMR: 300 MHz; ^{13}C NMR: 75 MHz) and JEOL ECX400II (^{1}H NMR: 400 MHz; ^{13}C NMR: 100 MHz) spectrometers with solvent resonance as chemical shift values with respect to chloroform (δ 7.26: ^{1}H NMR δ 77.16: ^{13}C NMR) and tetramethylsilane (δ 0.00: ^{1}H NMR, internal standard). High-resolution mass spectra (HRMS) were obtained using a JEOL JMS-AX500 with a field desorption (FD) probe at the positive mode using cholesterol as an internal standard. Current (I)–voltage (V) curves were obtained by high-resistance-low-current electrometer (KEYTHLEY 6517B), power supply (ADVANTEST R6142), scanner (ADVANTEST R7210), and a digital multimeter (KEYTHELY 2001). Differential scanning calorimetry

(DSC) was performed using a Diamond DSC (PerkinElmer, Inc.).

3. Materials

The following reagents were purchased from commercial suppliers and used as received: tetrahydrofuran (THF, superdehydrated, stabilized with 2,6-di-*t*-butyl-*p*-cresol, Wako Pure Chemical Industries), dichloromethane (superdehydrated, Wako Pure Chemical Industries), acetone (superdehydrated, Wako Pure Chemical Industries), *N*-bromosuccinimide (NBS, Wako Pure Chemical Industries), *n*-butyllithium (^{n}BuLi, 1.6 M in hexane, Kanto Chemical), dimethyl diselenide (Tokyo Chemical Industry), tetra-*n*-butylammonium hexafluoroborate (^{n}Bu$_4$N•BF$_4$, Tokyo Chemical Industry), tetra-*n*-butylammonium hexafluoroperchlorate (^{n}Bu$_4$N•ClO$_4$, Tokyo Chemical Industry) carbon paste (XC-12, DOTITE, Fujikura Kasei), silver paste (D-500, DOTITE, Fujikura Kasei), and ethylene glycol monobutyl ether acetate (Tokyo Chemical Industry). **2O**-2H,[S1] **2S**-2Br,[S2] and dimethyl ditelluride[S3] were synthesized according to literature procedure.

4. Synthesis

4-1. Synthesis of **2O**-2SeMe

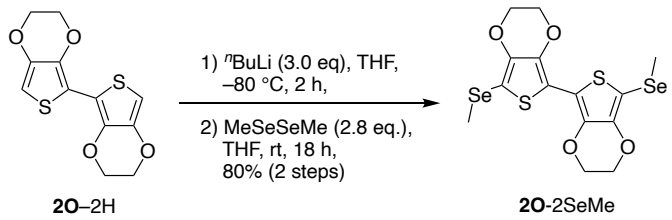

To a solution of **2O**-2H (100 mg, 354 μmol) in THF (6.0 mL) was dropwise added ^{n}BuLi (1.58 M in hexane, 0.70 mL, 1.06 mmol) at –80 °C, and the mixture was stirred for 2 h. To the solution was added dimethyl dimethyl diselenide (0.25 mL, 980 μmol) dropwise, and the mixture was allowed to warm to ambient temperature and stirred for 18 h. After the removal of the volatile materials in vacuo and the addition of saturated aqueous sodium bicarbonate (30 mL), the mixture was extracted with dichloromethane (50 mL). The combined organic layer was dried over sodium sulfate and concentrated in vacuo. The crude material was purified by preparative GPC eluted with chloroform to afford **2O**-2SeMe (132 mg, 282 μmol) as a white solid in a total yield of 80% for the 2-step transformations from **2O**-2H. The structural integrity of **2O**-2SeMe was confirmed by the XRD analysis of the single crystal obtained from recrystallization by liquid–liquid diffusion method using dichloromethane and ethanol as the solvents (Table S1, Fig. S3). Physical data of **2O**-2SeMe: ^{1}H NMR ($CDCl_3$, 300 MHz) δ 2.25 (s, 6H), 4.32 (s, 8H); ^{13}C NMR ($CDCl_3$, 75 MHz) δ 11.2, 64.9, 65.1, 96.9,

113.4, 136.9, 143.4; HRMS (FD$^+$) calcd for $C_{14}H_{14}O_4S_2Se_2$ [$M^{\bullet+}$] 469.8659, found 469.8649. The purity of the compound was confirmed by ^{1}H and ^{13}C NMR spectra (Fig. S18 and S19).

4-2. Synthesis of **2O**-2SeMe•*X* (*X* = BF_4, ClO_4)

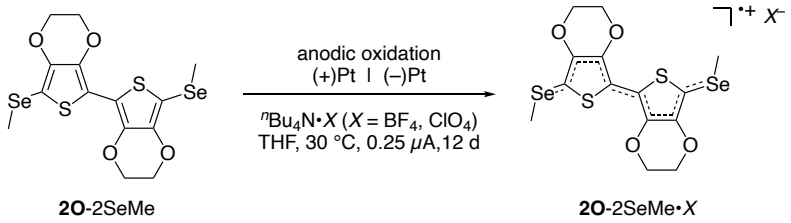

2O-2SeMe **2O**-2SeMe•*X*

Donor **2O**-2SeMe (1.0 mg, 1.2 μmol) was placed in one side of an H-shaped cell equipped with a glass filter and ^{n}Bu$_4$N•*X* (*X* = BF_4, ClO_4) (10 mg x 2) was placed in each side of the cell. The compounds were dissolved in degassed THF (10 mL) under ultrasonic irradiation for >1 h. Two pre-annealed platinum electrodes were inserted into each side of the cell, and the cell was kept at 30 °C for 1 h. Then, a constant current of 0.25 μA was applied to the solution at 30 °C for 12 d to afford black needle-like crystals of **2O**-2SeMe•*X* (*X* = BF_4, ClO_4). The crystal structures were identified by single-crystal X-ray structural analyses (Table S1 and Fig. S4 −S6).

4-3. Synthesis of **2S**-2TeMe

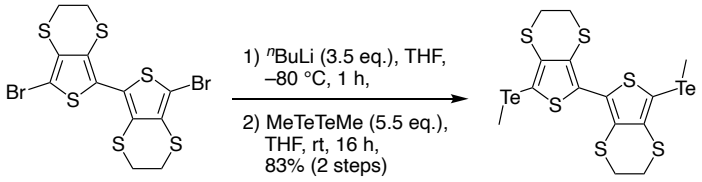

2 **2S**-2TeMe

To a solution of **2S**-2Br (250 mg, 496 μmol) in THF (50 mL) was dropwise added ^{n}BuLi (1.58 M in hexane, 1.10 mL, 1.49 mmol) at –80 °C, and the mixture was stirred for 1 h. To the solution was added dimethyl ditelluride (282 μL, 2.48 mmol) dropwise, and the mixture was allowed to warm to ambient temperature and stirred for 16 h. After the removal of the volatile materials in vacuo and the addition of saturated aqueous sodium bicarbonate (30 mL), the mixture was extracted with dichloromethane (60 mL). The combined organic layer was dried over sodium sulfate and concentrated in vacuo. The crude material was purified by preparative

GPC eluted with chloroform to afford **2S**-2TeMe (259 mg, 411 μmol) as a yellow solid in a total yield of 83% for the 2-step transformations from **2S**-2Br. Physical data of **2S**-2TeMe: ^{1}H NMR ($CDCl_3$, 400 MHz) δ 2.16 (s, 6H), 3.14-3.17 (m, 4H), 3.28-3.31 (m, 4H); ^{13}C NMR ($CDCl_3$, 100 MHz) δ −13.4, 28.1, 29.2, 94.5, 126.9, 132.3, 135.6; HRMS (FD^+) calcd for $C_{14}H_{14}S_6Te_2$ [$M^{\bullet+}$] 633.7506, found 633.7516. The purity of the compound was confirmed by ^{1}H and ^{13}C NMR spectra (Fig. S20 and S21).

5. DFT calculations for isolated molecules

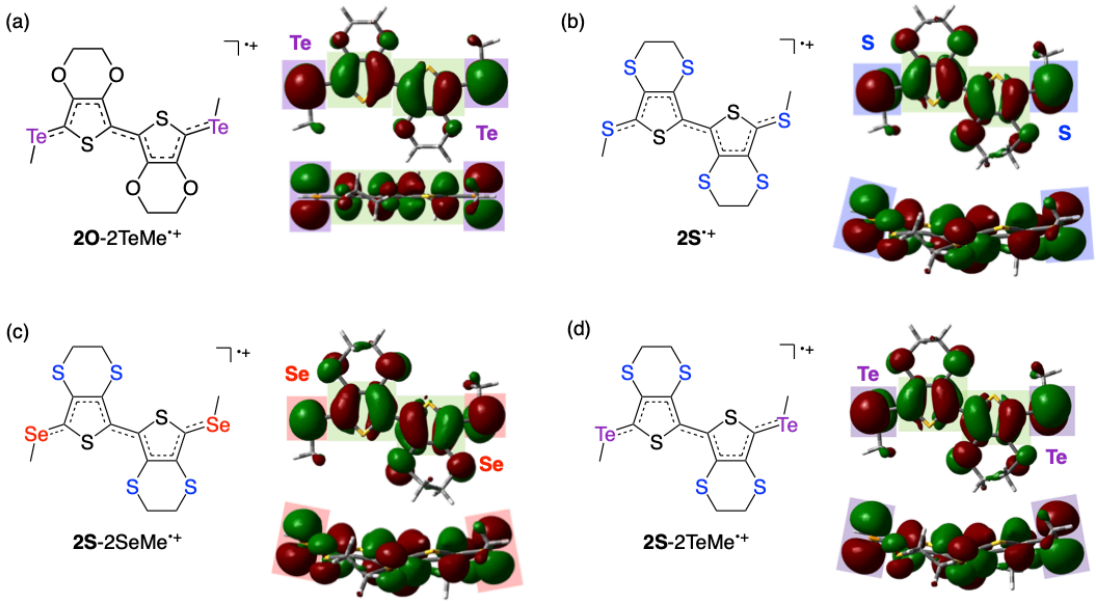

Fig. S1. Molecular structures and orbitals. (a) **2O**-2TeMe$^{\bullet+}$. (b) **2S**$^{\bullet+}$.[S2] (c) **2S**-2SeMe$^{\bullet+}$. (d) **2S**-2TeMe$^{\bullet+}$.

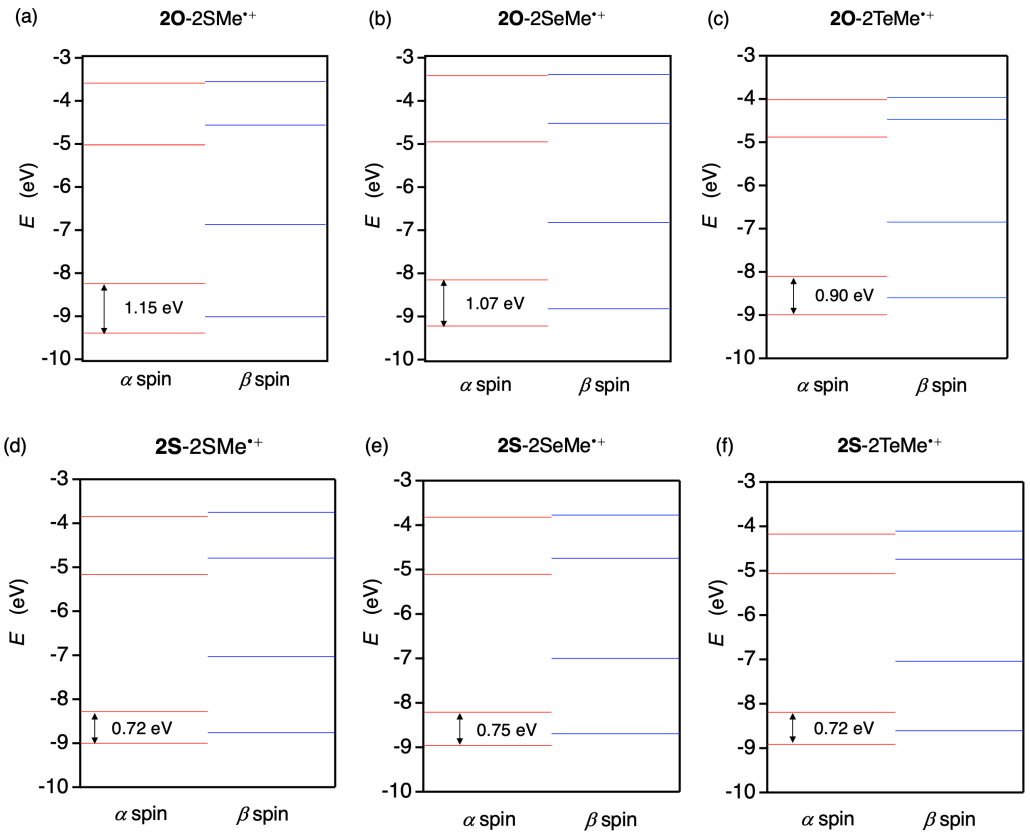

Fig. S2. Molecular orbital level of (a) **2O**$^{\bullet+}$,[S4] (b) **2O**-2SeMe$^{\bullet+}$, (c) **2O**-2TeMe$^{\bullet+}$, (d) **2S**$^{\bullet+}$,[S2] (e) **2S**-2SeMe$^{\bullet+}$, and (f) **2S**-2TeMe$^{\bullet+}$.

6. Single-crystal XRD structural analysis

Table S1. Crystallographic data for single crystals of **2O**-2SeMe, **2O**-2SeMe•BF_4, and **2O**-2SeMe•ClO_4.

Compounds	**2O**-2SeMe	**2O**-2SeMe•BF_4	**2O**-2SeMe•BF_4	**2O**-2SeMe•ClO_4	**2O**-2SeMe•ClO_4
Temperature / K	293	293	123	293	133
Formula	$C_{14}H_{14}O_4S_2Se_2$	$C_{14}H_{14}BF_4O_4S_2Se_2$	$C_{14}H_{14}BF_4O_4S_2Se_2$	$C_{14}H_{14}ClO_8S_2Se_2$	$C_{14}H_{14}ClO_8S_2Se_2$
Formula weight	468.29	555.10	555.10	566.73	535.69
Crystal system	triclinic	monoclinic	monoclinic	monoclinic	triclinic
Space group	*P*-1	*I*2/*a*	*Pc*	*Ia*	*P*-1
a / Å	5.0619(3)	7.1483(6)	6.9821(4)	7.1829(5)	7.0908(3)
b / Å	8.2779(5)	22.3136(15)	44.1634(19)	22.5481(13)	12.8737(7)
c / Å	10.5987(6)	11.9377(11)	11.9011(7)	12.0152(9)	21.0151(10)
α / deg.	74.788(5)	90	90	90	94.853(4)
β / deg.	79.994(5)	99.218(7)	97.465(5)	99.252(6)	92.065(4)
γ / deg.	73.339(5)	90	90	90	101.898(4)
V / Å^3	408.22(4)	1879.5(3)	3638.6(3)	1920.7(2)	1867.60(16)
Z	1	4	8	4	4
D_{calc} / g cm^{-3}	1.905	1.962	2.027	1.960	1.905
R_{int}	0.0375	0.0510	0.0965	0.0202	0.0503
R_1 ($I > 2.00\sigma(I)$)	0.0409	0.0439	0.1229	0.0307	0.0996
wR_2 (all reflections)	0.1043	0.1180	0.3401	0.0685	0.2287
GOF	1.037	1.095	0.986	1.041	1.142
CCDC	2349871	2349872	2352190	2349870	2352192

The single-crystal structures of **2O**-2SeMe and **2O** were compared. The SeMe of **2O**-2SeMe are located perpendicular to the thiophene ring at an angle of 64.1(4)°. The SMe of **2O** groups 78(1)°, 88.1(2)° and 95.7(8)° for **2O**.[S4] The dihedral angle between the two thiophene rings was 180.0(4)° for **2O**-2SeMe, and 180.0(1)° and 180.0(2)° for **2O**,[S4] respectively. No disorder of ethylenedioxy groups was observed in **2O**-2SeMe (Fig. S3), while disorder of ethylenedioxy groups was observed in **2O**.[S4]

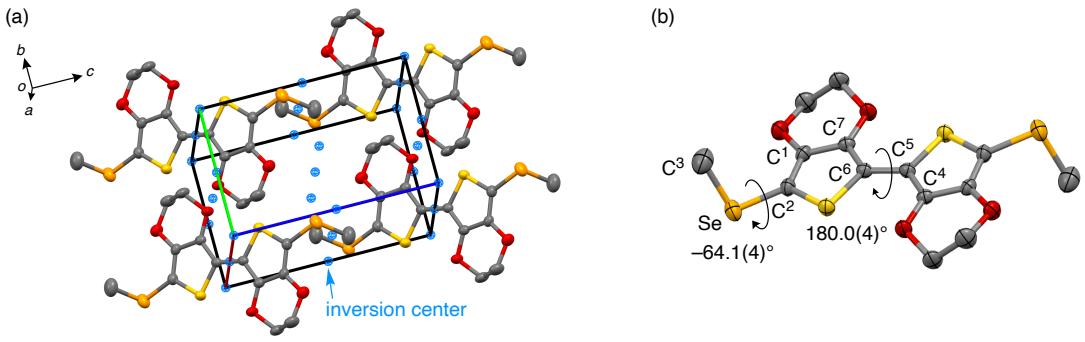

Fig. S3. The single-crystal structure of **2O**-2SeMe in ORTEP drawing (50% thermal ellipsoids). (a) The symmetry elements for the packing structure. (b) The molecular structure. The twisting angle between end group and thiophene ring was defined as the angle C^1–C^2–Se–C^3; the twisting angle between the two thiophene rings was defined as the dihedral angle C^4-C^5-C^6-C^7. Hydrogen atoms were omitted for clarity. Yellow: S, red: O, grey: C, orange: Se.

In the **2O**-2SeMe•BF_4 crystal, the ethylenedioxy groups in **2O**-2SeMe were disordered with a ratio of 0.42:0.58. In addition, the counter anion BF_4^- was also disordered in a ratio of 0.50:0.50 (Fig. S4).

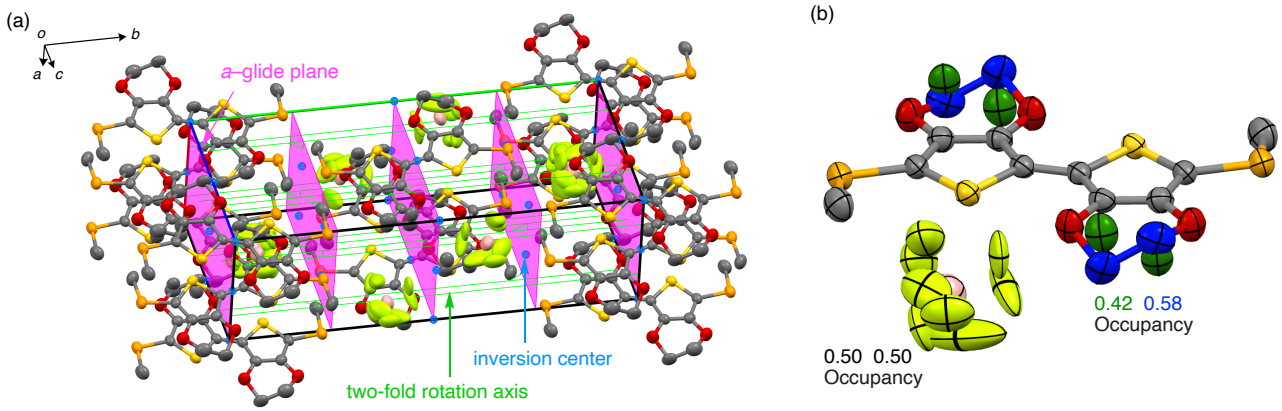

Fig. S4. The crystal structure **2O**-2SeMe•BF_4 at 293 K in ORTEP drawing (50% thermal ellipsoids). (a) The packing structure with the symmetry elements. (b) The molecular structure with disordered atoms depicted in bule and green colors with the occupancies. Hydrogen atoms were omitted for clarity. Yellow: S, red: O, gray: C, yellowish green: F, orange: Se, pink: B.

In the **2O**-2SeMe•ClO_4 crystal, the ethylenedioxy groups in **2O**-2SeMe were disordered with a ratio of 0.42:0.58 and 0.46:0.54 respectively. In addition, the counter anion ClO_4^- was also disordered in a ratio of 0.42:0.58 (Fig. S5).

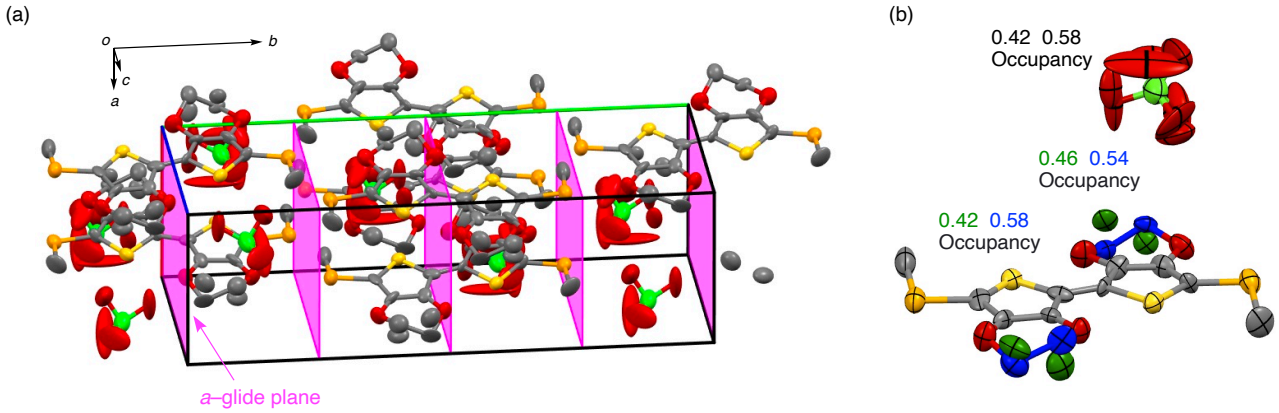

Fig. S5. The crystal structure **2O**-2SeMe•ClO_4 at 293 K in ORTEP drawing (50% thermal ellipsoids). (a) The packing structure with the symmetry elements. (b) Disordered atoms were depicted in bule and green colors with the occupancies. Hydrogen atoms were omitted for clarity. Yellow: S, red: O, gray: C, light green: Cl, orange: Se.

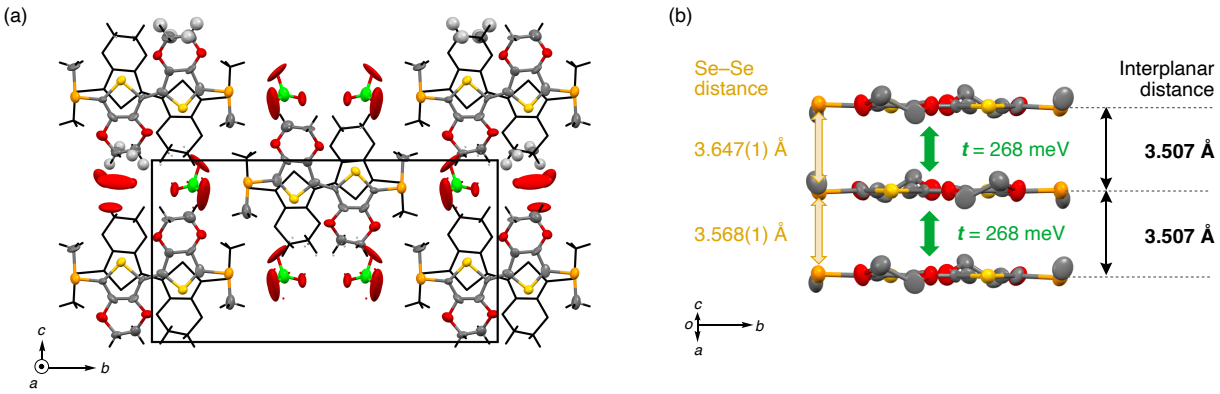

Fig. S6. Single-crystal structures **2O**-2SeMe•ClO_4 at 293 K in ORTEP drawing (50% thermal ellipsoids) along (a) the *a*-axis and (b) the direction perpendicular to the molecular plane. [a]The interplanar distances were measured between the geometric center of the bithiophene atoms in **2O**–2SeMe and the mean plane composed of bithiophene ten atoms in the facing donor. Green arrows represent transfer integrals (***t***) for the intracolumnar interactions between the two nearest molecules. Hydrogens are omitted for clarity in (b). Yellow: S, green: Cl,

red: O, grey: C, light gray: H, orange: Se.

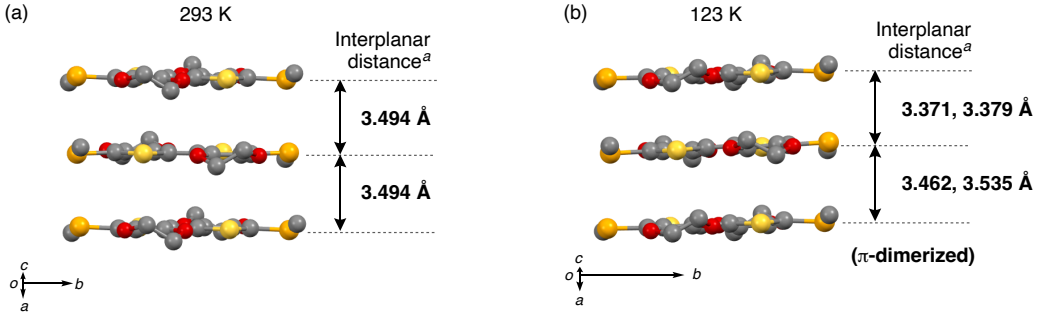

Fig. S7. The packing structure of **2O**-2SeMe•BF_4 at 123 K with bold and stick model. Hydrogen atoms were omitted for clarity. Yellow: S, red: O, gray: C, orange: Se. [a]The interplanar distances were measured between the geometric center of the bithiophene atoms in **2O**–2SeMe and the mean plane composed of bithiophene ten atoms in the facing donor.

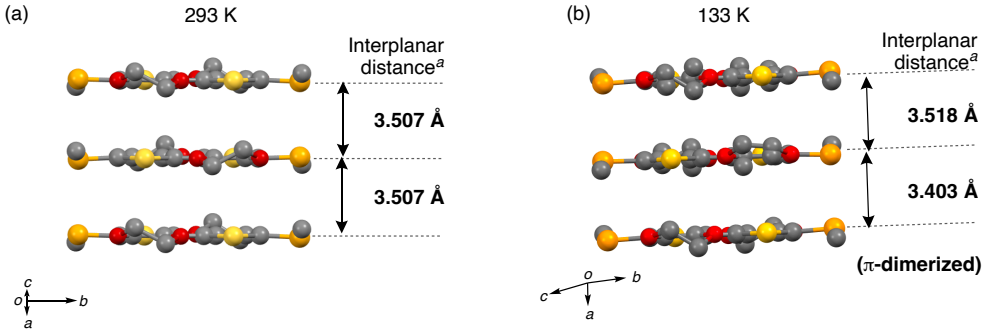

Fig. S8. The packing structure of **2O**-2SeMe•ClO_4 at 133 K with bold and stick model. Hydrogen atoms were omitted for clarity. Yellow: S, red: O, gray: C, orange: Se. [a]The interplanar distances were measured between the geometric center of the bithiophene atoms in **2O**–2SeMe and the mean plane composed of bithiophene ten atoms in the facing donor.

7. Theoretical calculations

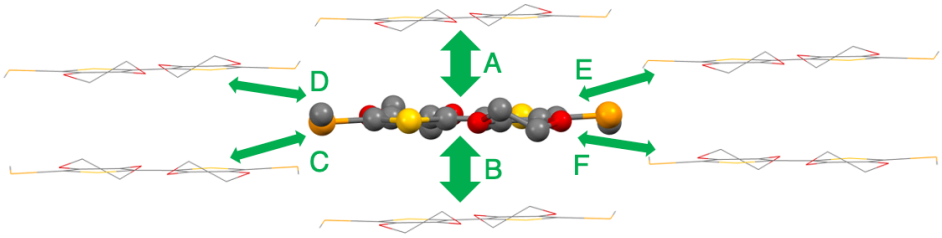

Fig. S9. Labels for transfer integral. The values are summarized in Table S2. Yellow: S, red: O, grey: C, orange:

Se.

Table S2. Transfer integrals for **2O**•BF_4, **2O**•ClO_4, **2O**-2SeMe•BF_4, and **2O**-2SeMe•ClO_4.

Transfer integral (meV)		**2O**•BF_4	**2O**•ClO_4	**2O**-2SeMe•BF_4	**2O**-2SeMe•ClO_4
t_{intra}					
	A	238	250	285	268
	B	238	250	285	268
t_{inter}					
	C	0.24	0.36	0.39	0.86
	D	0.24	0.27	0.23	0.11
	E	0.24	0.36	0.39	0.86
	F	0.24	0.27	0.39	0.11

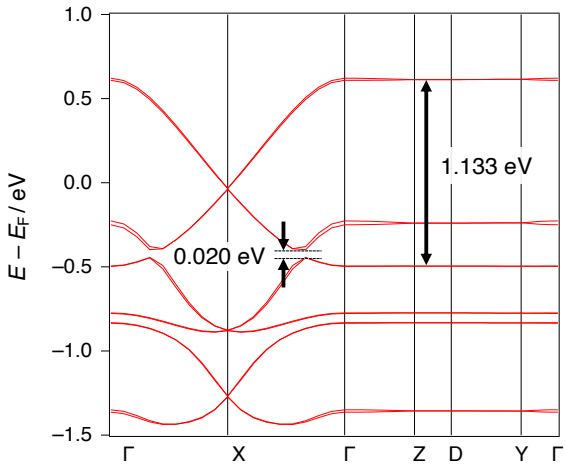

Fig. S10. Band dispersion of **2O**-2SeMe•ClO_4. Γ (0,0,0), X (0.5,0,0), Z (0,0.5,–0.5), D (0.0,0.5,0.5), Y (0,0.5,0). The bandgap was determined by the density of states (DOS) (Fig. S12b).

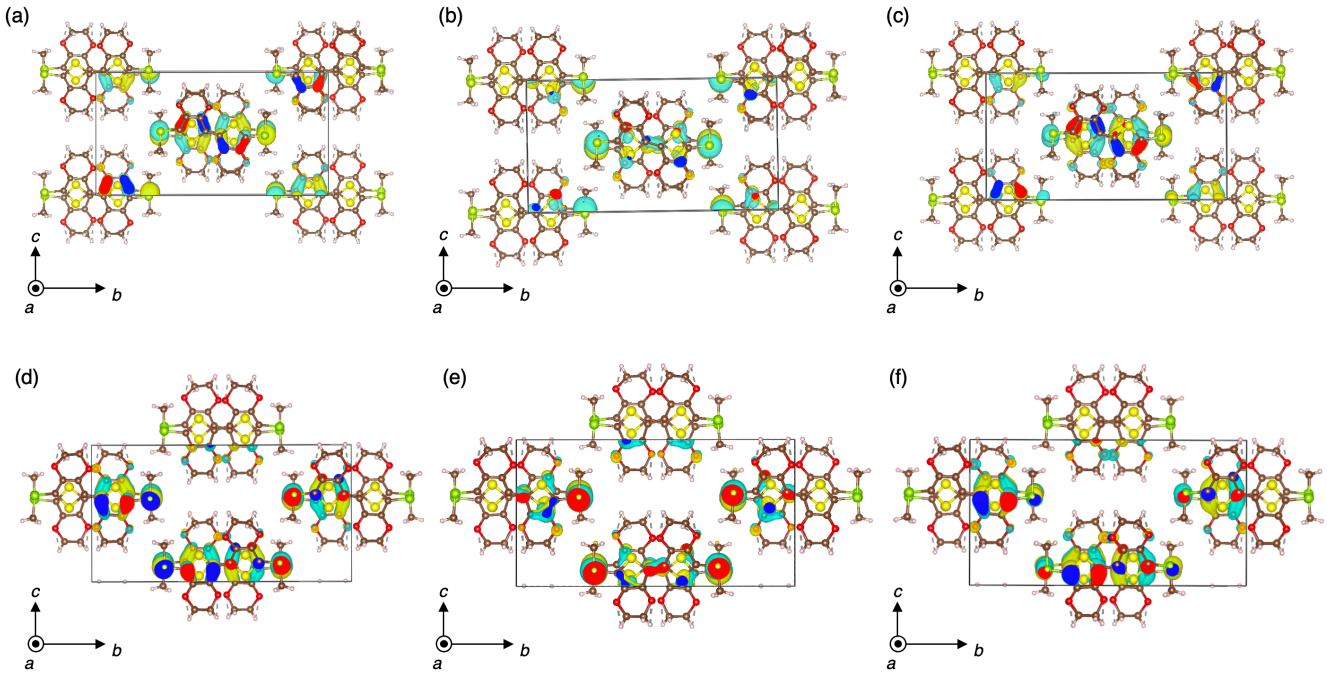

Fig. S11. LUCO of (a) **2O**-2SeMe•BF_4 and (d) **2O**-2SeMe•ClO_4. HOCO of (b) **2O**-2SeMe•BF_4 and (e) **2O**-2SeMe•ClO_4. HOCO−1 of (c) **2O**-2SeMe•BF_4 and (f) **2O**-2SeMe•ClO_4 at the Γ point (0,0,0). Yellow: S; red: O; gray: C; green; pink: Se; white: H.

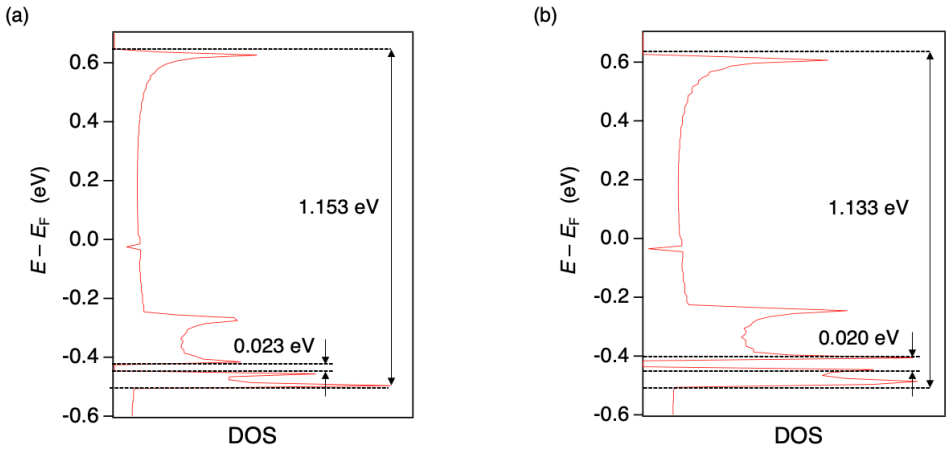

Fig. S12. DOS of (a) **2O**-2SeMe•BF_4 and (b) **2O**-2SeMe•ClO_4.

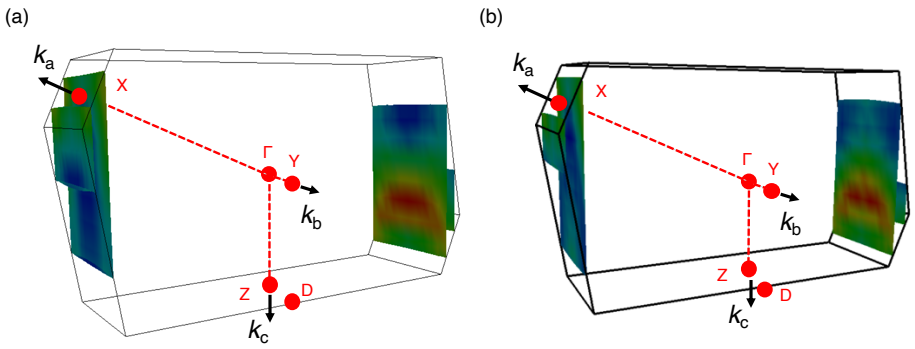

Fig. S13. The Fermi surface and the first Brillouin zone of (a) **2O**-2SeMe•BF_4 and (b) **2O**-2SeMe•ClO_4.

8. Static magnetic susceptibility measurements

The contribution from core diamagnetism (**2O**-2SeMe•BF_4: $\chi_{core} = -2.73 \times 10^{-4}$ emu mol^{-1} and **2O**-2SeMe•ClO_4: -2.73×10^{-4} emu mol^{-1}) are estimated from Pascal's law.[S5]

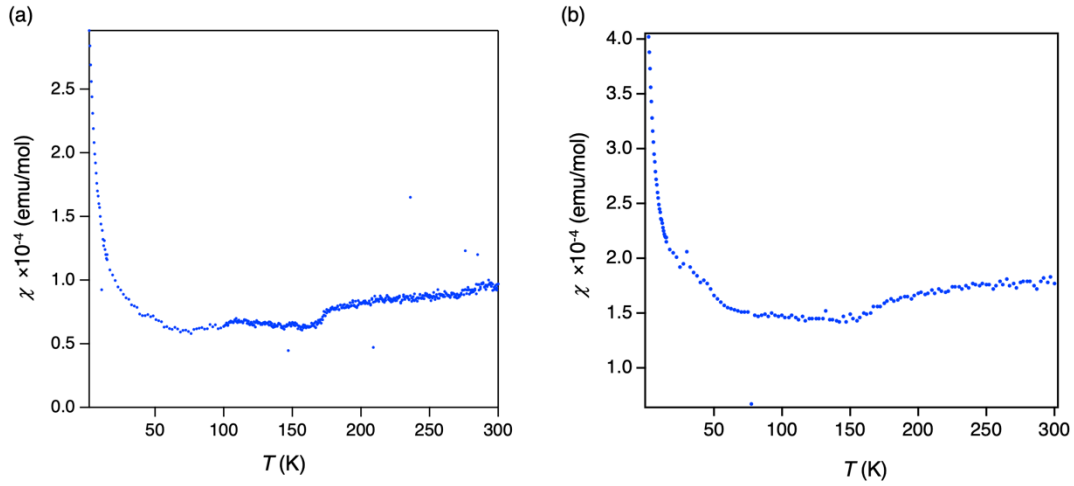

Fig. S14. χ–T plots of poly crystals (a) **2O**-2SeMe•BF_4 and (b) **2O**-2SeMe•ClO_4.

9. Electrical resistivity measurement

Ohmic behavior of the sample was confirmed by the current–voltage (*I–V*) measurement (Fig. S15).

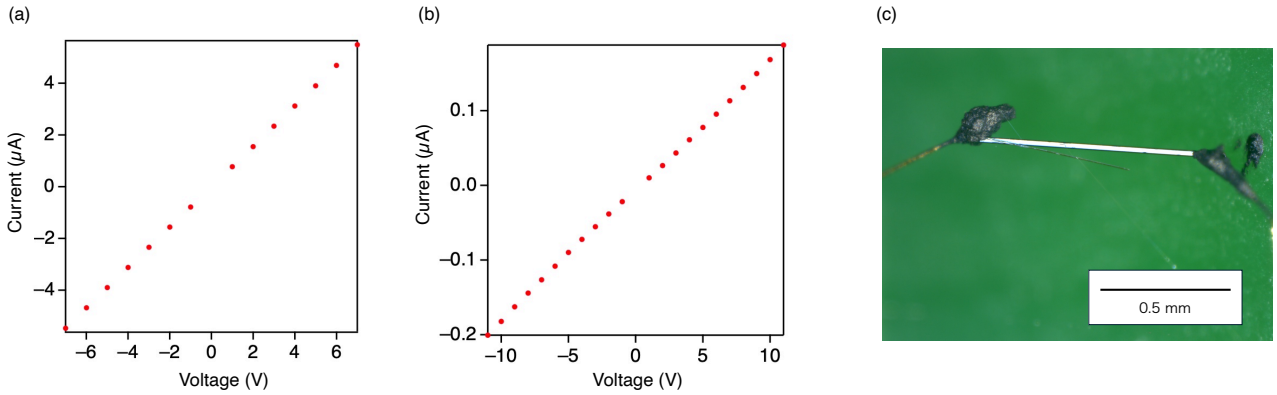

Fig. S15. *I–V* curve of (a) **2O**-2SeMe•BF_4 and (b) **2O**-2SeMe•ClO_4 at 293 K. (c) The picture of single crystal 2O-2SeMe•BF_4 used in the measurement.

10. DSC measurements

Al pans were filled with 3.08 mg samples for differential scanning calorimetry (DSC) measurement. The results are shown in Fig. S16. The data of an empty Al pan measured under the same conditions were subtracted from the sample measurement data, and the background was subtracted. Thermodynamic parameters were obtained from DSC measurements. (ΔH = 326 J mol^{-1} and ΔS = 2.04 J mK^{-1} mol^{-1})

The exothermic peak was observed at 150−180 K for **2O**-2SeMe•BF_4 polycrystals, which is consistent to the transition temperature of the resistivity at approximately 170 K for the single crystal (Fig. 6) and the magnetic susceptibility at approximately 170 K for the polycrystals (Fig. S14a). This transition might be related to the donor dimerization indicated by the crystal structure analyses at 293 K and 123 K owing to the 1D electronic structure.

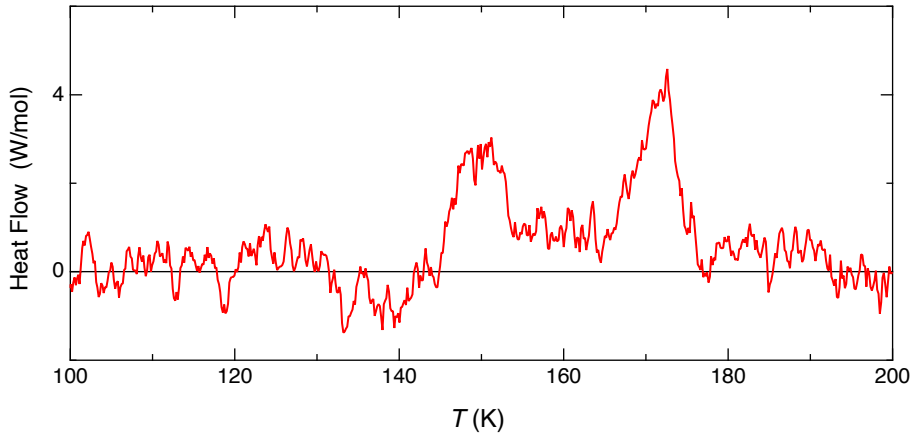

Fig. S16. DSC charts of **2O**-2SeMe•BF_4 polycrystals.

Al pans were filled with 4.57 mg samples for measurement. The results are shown in Fig. S17. The data of an empty Al pan measured under the same conditions were subtracted from the sample measurement data, and the background was subtracted. Thermodynamic parameters were obtained from DSC measurements (ΔH = 958 J mol^{-1} and ΔS = 5.99 J mK^{-1} mol^{-1}).

The exothermic peak was observed at 150−170 K for **2O**-2SeMe•ClO_4 polycrystals, which is consistent to the gradual decrease of the magnetic susceptibility at 150–170 K (Fig. S14b). This transition might be related to the donor dimerization indicated by the crystal structure analyses at 293 K and 133 K owing to the 1D electronic structure.

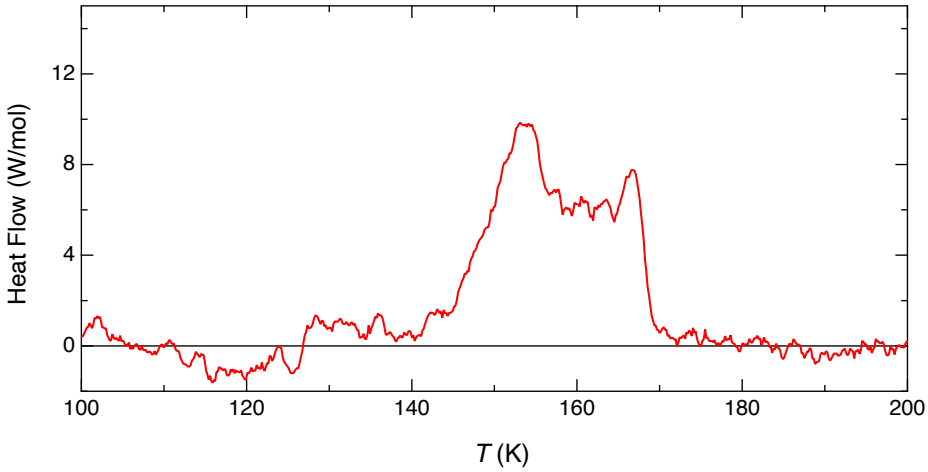

Fig. S17. DSC charts of **2O**-2SeMe•ClO_4 polycrystals.

11. Coordinates of DFT-optimized structures

Table S3. The geometry of optimized structure for radical cation **2O**-2SeMe$^{\bullet+}$.

C	3.26958916	4.18592844	0.43195322
C	2.96812055	5.47315667	0.91864838
C	3.59532936	5.78514936	2.13161619
C	2.25251514	7.69382275	0.76786176
H	3.15390880	8.14788969	0.34091960
H	1.36729454	8.21032446	0.39351012
C	2.29897829	7.71317884	2.28844601
H	1.38560305	7.28082351	2.71451463
H	2.42705133	8.73163363	2.65932225
O	2.15066028	6.33286729	0.27222915
O	3.43544718	6.96750295	2.77401830
S	4.39168152	3.37923067	1.55152786
C	2.80892709	3.58251469	–0.74864843
C	3.11039574	2.29528660	–1.23534376
C	2.48318639	1.98329342	–2.44831106
C	3.82599217	0.07461916	–1.08455290
H	2.92459414	–0.37943960	–0.65761106
H	4.71120799	–0.44188835	–0.71019802
C	3.77953154	0.05525857	–2.60513710
H	4.69291013	0.48760689	–3.03120555
H	3.65145257	–0.96319651	–2.97601064
O	3.92785655	1.43557542	–0.58892512
O	2.64306832	0.80094049	–3.09071398
S	1.68683454	4.38921234	–1.86822288
C	1.66696037	3.00252263	–2.93117911
C	4.41155478	4.76592015	2.61448462
C	–0.18548150	4.57982070	–4.58734019
H	–0.78141481	4.55777554	–5.50192026
H	–0.84157437	4.70424793	–3.72415246

H	0.55210656	5.38179205	–4.64837444
C	6.26399085	3.18861898	4.27064965
H	6.85993561	3.21066957	5.18522214
H	5.52640032	2.38665111	4.33169957
H	6.92007290	3.06418185	3.40745512
Se	5.36430798	4.94682039	4.20247935
Se	0.71420685	2.82162194	–4.51917338

Table S4. The geometry of optimized structure for radical cation **2O**-2TeMe$^{\bullet+}$.

C	3.23368231	4.42606472	0.44217755
C	2.67960538	5.71727645	0.53775644
C	3.07609942	6.42566265	1.68385810
C	1.65011894	7.65962679	–0.26342072
H	2.51618523	8.16363483	–0.70719208
H	0.75401679	7.89024636	–0.84184848
C	1.47852984	8.05168124	1.19672776
H	0.59928021	7.56249477	1.63316257
H	1.38193448	9.13395011	1.29950350
S	4.28864890	4.13925175	1.84141854
C	3.03675469	3.47802704	–0.57819945
C	3.59083308	2.18681627	–0.67378509
C	3.19432797	1.47843274	–1.81988505
C	4.62049120	0.24449427	0.12730940
H	3.75450920	-0.25963158	0.57110967
H	5.51665800	0.01395559	0.70566908
C	4.79202441	-0.14746229	–1.33287262
H	5.67116003	0.34189520	–1.76934801
H	4.88878855	-1.22970848	–1.43572204
S	1.98178469	3.76484296	–1.97743815
C	2.31715038	2.18334653	–2.63833047
C	3.95327186	5.72074500	2.50231041
C	5.88914148	4.73839148	4.77632213

H	5.23705328	3.87426634	4.91273672
H	6.64000028	4.55090764	4.00707973
H	6.38788823	4.96886031	5.72057439
C	0.38123397	3.16569175	–4.91231506
H	1.03332214	4.02981249	–5.04875454
H	–0.11753671	2.93521018	–5.85655114
H	–0.36960091	3.35317900	–4.14305064
Te	1.54772116	1.42265370	–4.40723259
Te	4.72267134	6.48142539	4.27122971
O	3.62565366	0.22180070	–2.09874703
O	4.42846322	1.67628138	0.25538295
O	1.84198622	6.22781682	–0.39141106
O	2.64477625	7.68228203	1.96273532

Table S5. The geometry of optimized structure for radical cation **2S**-2SeMe$^{\bullet+}$.

C	3.26742200	4.17153100	0.42201600
C	2.96629000	5.48542000	0.92047500
C	3.58863300	5.78318600	2.12081300
C	2.25101800	7.71210900	0.78275400
H	3.13909000	8.17469100	0.34166500
H	1.35135800	8.20766900	0.41714700
C	2.30705200	7.71899600	2.30258300
H	1.39631500	7.29874900	2.74225000
H	2.46262800	8.73109200	2.67856400
O	2.17530100	6.33840500	0.26865800
O	3.43872800	6.93990100	2.78003900
S	4.39553700	3.34488100	1.54484200
C	2.81108800	3.59690800	–0.73870800
C	3.11222200	2.28302000	–1.23716800
C	2.48987700	1.98525300	–2.43750500
C	3.82749800	0.05633200	–1.09945000
H	2.93942500	–0.40624900	–0.65836200

H	4.72715700	–0.43922900	–0.73384300
C	3.77146400	0.04944700	–2.61927900
H	4.68219800	0.46969900	–3.05894500
H	3.61589200	–0.96264800	–2.99526300
O	3.90321500	1.43003700	–0.58535400
O	2.63978400	0.82853900	–3.09673300
S	1.68296300	4.42355300	–1.86152700
C	1.66546100	3.03111600	–2.91787600
C	4.41304500	4.73732200	2.60118600
C	–0.19376600	4.56940200	–4.61115700
H	–0.77811600	4.50012700	–5.53101000
H	–0.86013800	4.69845400	–3.75628400
H	0.53446900	5.37827100	–4.69317800
C	6.27227200	3.19903600	4.29446800
H	6.85660300	3.26830300	5.21433500
H	5.54403600	2.39016700	4.37646700
H	6.93866200	3.06999300	3.43960700
Se	5.33771500	4.93735900	4.16471800
Se	0.74079500	2.83108100	–4.48140900

Table S6. The geometry of optimized structure for radical cation **2S**-2TeMe$^{\bullet+}$.

C	3.32126242	4.19247769	0.43381825
C	3.03297769	5.42991128	0.95943115
C	3.68474320	5.70847158	2.18137239
C	2.25333213	7.60257824	0.95720276
H	2.90085484	8.13319385	0.46686576
H	1.38756669	8.01722741	0.81880123
C	2.54995739	7.71810874	2.27100440
H	1.73024514	7.57145043	2.76833555
H	2.81518960	8.63819681	2.42816295
S	4.40710200	3.36140163	1.48975268
C	2.84091479	3.61952314	-0.80263297

C	3.12919952	2.38208954	-1.32824587
C	2.47743401	2.10352924	-2.55018710
C	3.90884512	0.20942358	-1.32601755
H	3.26132237	-0.32119303	-0.83568048
H	4.77461052	-0.20522659	-1.18761594
C	3.61221986	0.09389308	-2.63981919
H	4.43193207	0.24055040	-3.13715027
H	3.34698761	-0.82619599	-2.79697767
S	1.75507521	4.45059920	-1.85856740
C	1.69090664	3.14174082	-2.97729119
C	4.47127057	4.67026001	2.60847647
C	6.05535667	3.33487591	4.45900770
H	5.35658525	2.52620805	4.51072621
H	6.78732961	3.12620856	3.70696145
H	6.53971325	3.44885323	5.40627106
C	-0.20881862	4.31301244	-4.63144112
H	0.39772084	5.18819613	-4.73662377
H	-0.76923453	4.15740374	-5.52956134
H	-0.88130845	4.44183416	-3.80921099
O	2.61334740	0.92765384	-3.21250120
O	3.95402064	1.48927144	-0.71010650
O	2.20815657	6.32272939	0.34129179
O	3.54882981	6.88434698	2.84368648
Te	0.83317429	2.90166029	-4.33021712
Te	5.19437183	4.83765883	4.04821750

Table S7. The geometry of optimized structure for neutral **2O**-2SeMe.

C	3.09691300	3.88637900	0.61745700
C	2.78798100	5.08939400	1.22585700
C	3.48863600	5.32451800	2.44476400
C	4.34342100	4.30575200	2.78793200
C	2.03983200	7.29915900	1.27387900

H	2.92678300	7.77737300	0.83640900
H	1.14599600	7.85624000	0.98310000
C	2.16922500	7.22277900	2.78762300
H	1.27503600	6.75471900	3.22217100
H	2.30043000	8.21827700	3.21926600
O	1.88572300	5.98521000	0.71509700
O	3.33123100	6.47221500	3.16736300
S	4.29049400	3.03159300	1.59082600
C	2.57346100	3.35977000	-0.61745700
C	2.88239300	2.15675600	-1.22585700
C	2.18173800	1.92163100	-2.44476500
C	1.32695300	2.94039800	-2.78793200
C	3.63054200	-0.05301000	-1.27387900
H	2.74359100	-0.53122300	-0.83640900
H	4.52437800	-0.61009000	-0.98310000
C	3.50114900	0.02337100	-2.78762300
H	4.39533800	0.49143000	-3.22217100
H	3.36994400	-0.97212700	-3.21926600
O	3.78465200	1.26094000	-0.71509700
O	2.33914300	0.77393400	-3.16736300
S	1.37988000	4.21455700	-1.59082700
C	1.31056100	3.74839400	-5.61464900
H	2.12590500	3.05481100	-5.82557700
H	0.70236200	3.89727400	-6.51103300
H	1.69923600	4.70499600	-5.26186500
C	4.35981300	3.49775500	5.61464800
H	4.96801200	3.34887500	6.51103200
H	3.54446900	4.19133800	5.82557700
H	3.97113800	2.54115300	5.26186400
Se	5.56168000	4.27429800	4.22858100
Se	0.10869300	2.97185200	-4.22858100

Table S8. The geometry of optimized structure for dication **2O**-2SeMe^{2+}.

C	3.26742200	4.17153100	0.42201600
C	2.96629000	5.48542000	0.92047500
C	3.58863300	5.78318600	2.12081300
C	2.25101800	7.71210900	0.78275400
H	3.13909000	8.17469100	0.34166500
H	1.35135800	8.20766900	0.41714700
C	2.30705200	7.71899600	2.30258300
H	1.39631500	7.29874900	2.74225000
H	2.46262800	8.73109200	2.67856400
O	2.17530100	6.33840500	0.26865800
O	3.43872800	6.93990100	2.78003900
S	4.39553700	3.34488100	1.54484200
C	2.81108800	3.59690800	-0.73870800
C	3.11222200	2.28302000	-1.23716800
C	2.48987700	1.98525300	-2.43750500
C	3.82749800	0.05633200	-1.09945000
H	2.93942500	-0.40624900	-0.65836200
H	4.72715700	-0.43922900	-0.73384300
C	3.77146400	0.04944700	-2.61927900
H	4.68219800	0.46969900	-3.05894500
H	3.61589200	-0.96264800	-2.99526300
O	3.90321500	1.43003700	-0.58535400
O	2.63978400	0.82853900	-3.09673300
S	1.68296300	4.42355300	-1.86152700
C	1.66546100	3.03111600	-2.91787600
C	4.41304500	4.73732200	2.60118600
C	-0.19376600	4.56940200	-4.61115700
H	-0.77811600	4.50012700	-5.53101000
H	-0.86013800	4.69845400	-3.75628400
H	0.53446900	5.37827100	-4.69317800

C	6.27227200	3.19903600	4.29446800
H	6.85660300	3.26830300	5.21433500
H	5.54403600	2.39016700	4.37646700
H	6.93866200	3.06999300	3.43960700
Se	5.33771500	4.93735900	4.16471800
Se	0.74079500	2.83108100	-4.48140900

12. NMR spectra

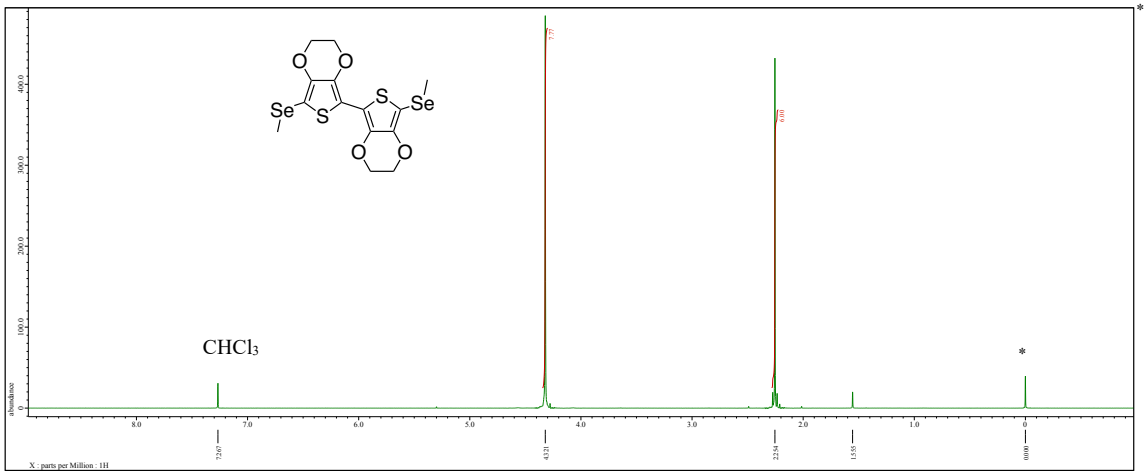

Fig. S18. ^{1}H NMR spectrum of **2O**-2SeMe in $CDCl_3$. The signal for $Si(CH_3)_4$ used for the internal standard was shown with an asterisk.

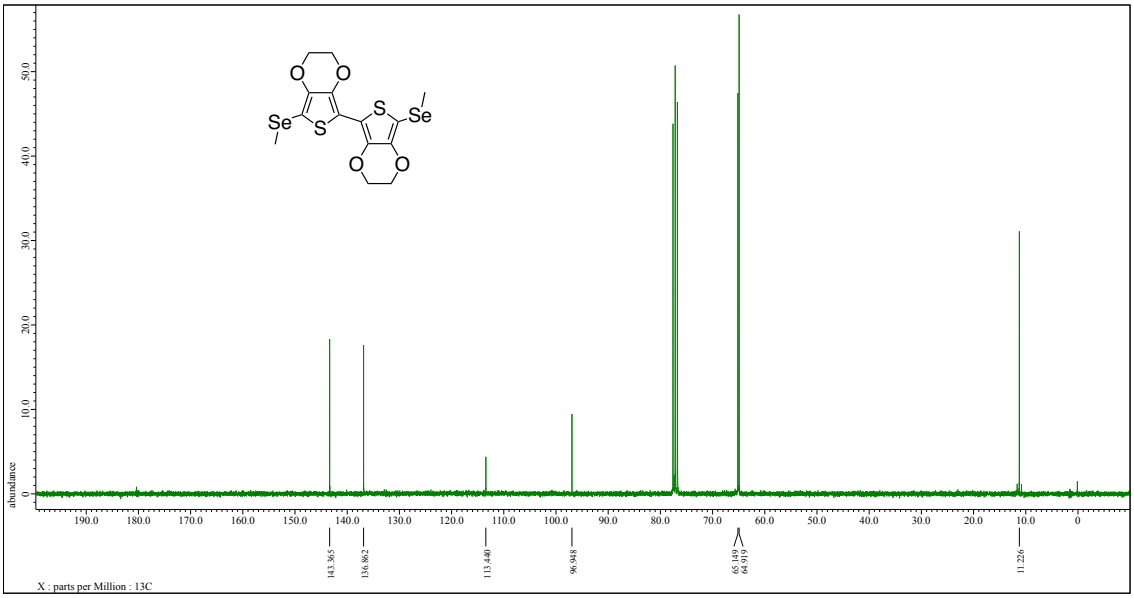

Fig. S19. ^{13}C NMR spectrum of **2O**-2SeMe in $CDCl_3$.

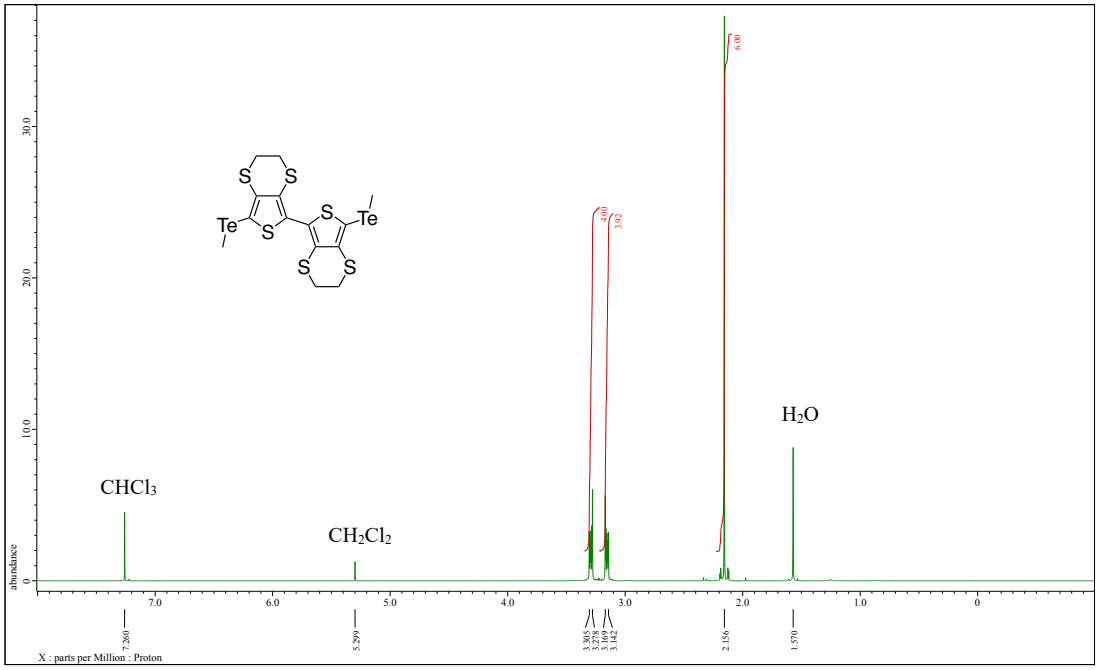

Fig. S20. ^{1}H NMR spectrum of **2S**-2TeMe in $CDCl_3$.

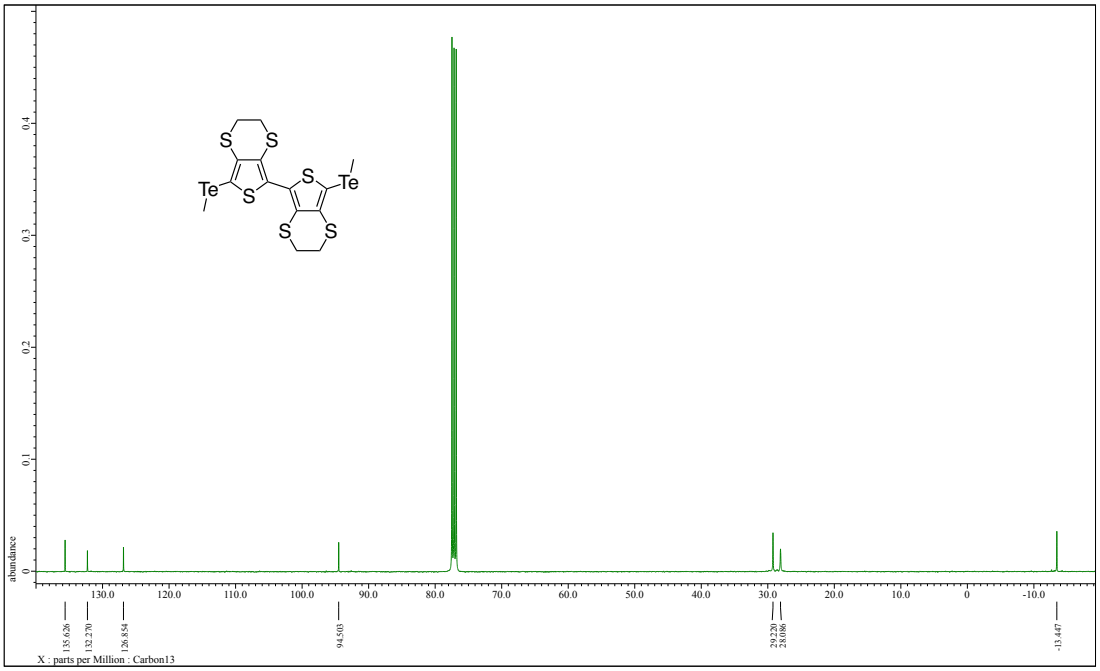

Fig. S21. ^{13}C NMR spectrum of **2S**-2TeMe in $CDCl_3$.

S1. A. Donat-Bouillud, I. Lévesque, Y. Tao, M. D'Iorio, S. Beaupré, P. Blondin, M. Ranger, J. Bouchard and M. Leclerc, *Chem. Mater.* 2000, **12**, 1931-1936.

S2. T. Fujino, R. Kameyama, K. Onozuka, K. Matsuo, S. Dekura, T. Miyamoto, Z. Guo, H. Okamoto, T. Nakamura, K. Yoshimi, S. Kitou, T. Arima, H. Sato, K. Yamamoto, A. Takahashi, H. Sawa, Y. Nakamura and H. Mori, *Nature Commun.* in press. DOI: 10.1038/s41467-024-47298-1.

S3. S. Yamago, K. Iida and J. Yoshida, *J. Am. Chem. Soc.*, 2002, **124**, 13666-13667.

S4 R. Kameyama, T. Fujino, S. Dekura, M. Kawamura, T. Ozaki and H. Mori, *Chem. Eur. J.* 2021, **27**, 6696-6700.

S5. G. A. Bain and J. F. Berry, Diamagnetic Corrections and Pascal's Constants. *J. Chem. Educ.* 2008, **85**, 532-536.